Journal of Green Chemical and Environmental Engineering

e-ISSN 3090-2568
p-ISSN 3109-2233

Research Paper

Enhanced Removal of Malachite Green Dye from Textile Wastewater using TiO_2 Modified Palm Kernel Shell Activated Carbon: Optimization and Mechanistic Assessment

Olowonyo Idayat A[1,*], Sole-Adeoye Opeoluwa D[1], Salam Kazeem K[2], Aremu Mujidat O[2], Oreofe Toyin A[3], Akinwumi Odunayo D[2], Owolabi Stephen O[4]

[1]Department of Chemical Engineering, Faculty of Engineering, Adeleke University, Ede, Osun State, Nigeria
[2]Department of Chemical Engineering, Faculty of Engineering and Tecnology, Ladoke Akintola Univ. of Technology, Ogbomoso, Oyo State, Nigeria
[3]Department of Chemical Engineering, College of Engineering, Landmark University, Omu aran, Kwara State, Nigeria
[4] Department of Civil Engineering, Faculty of Engineering, Adeleke University, Ede, Osun State, Nigeria

** Corresponding author: olowonyo.idayat@adelekeuniversity.edu.ng (Olowonyo I.A)*

Received 06 July 2025
Revised 25 August 2025
Accepted 16 Sept 2025

Citation: A. Olowonyo Idayat, D. Sole-Adeoye Opeoluwa, K. Salam Kazeem, O. Aremu Mujidat, O. Owolabi Stephen (2025). "Enhanced Removal of Malachite Green Dye from Textile Wastewater using TiO_2-Modified Palm Kernel Shell Activated Carbon: Optimization and Mechanistic Assessment". J. of Green Chemical and Environmental Engineering, Vol. 1, No. 3, Page 126-139.

: 10.63288/jgcee.v1i3.11

Abstract: Malachite Green Dye (MGD), a toxic dye commonly discharged by textile industries, poses environmental and health risks. Simultaneously, the disposal of palm kernel shells (PKS), a byproduct of palm oil production, remains an underexploited resource. This study explores the use of activated carbon derived from PKS, modified with titanium dioxide nanoparticles (TiO2-NP), for the adsorption of malachite green dye from aqueous solution. The adsorbent was characterized for its structural and surface chemistry. Batch adsorption experiments were carried out to evaluate the effects of dosage (0.5-2.5 g), contact time (30-150 min), agitation (100-300 rpm), and temperature (30-60 °C). Process optimization was carried out using the Box-Behnken design under the Response Surface Methodology (RSM) framework. Additionally, kinetic and thermodynamic analyses were performed to gain insights into the adsorption mechanism. Numerical optimization revealed a maximum dye removal of 92.6%. Kinetic analysis supported pseudo-second-order behavior, indicating chemisorption, while thermodynamic data confirmed a spontaneous and endothermic process. The adsorbent showed effective regeneration over five cycles, maintaining high efficiency. The prepared adsorbent exhibited a fixed carbon content of 69.50%, while the presence of functional groups involved in dye binding was confirmed through FTIR analysis. These results underscore the potential of PKSAC-TiO_2 as a cost-effective and sustainable adsorbent for dye-laden wastewater treatment.

Keywords: Textile wastewater; Malachite green dye; Adsorption; Nanocomposite; Response Surface Methodology

1. Introduction

Textile manufacturing is a major water consumer and pollutant emitter, particularly through dyes like malachite green dye (MGD), known for their toxicity and resistance to degradation. Exposure to MGD can result in adverse health outcomes, including skin irritation, respiratory issues, and mutagenicity. Therefore, it is highly important to reduce the concentrations of MGD in wastewater before discharging into waterbodies [1], [2].

Numerous treatment technologies such as adsorption, electrochemical oxidation, photocatalysis, filtration and ozonation have been explored for dye removal [3], [4], [5]. Among all, adsorption process is considered a reliable and efficient technique for decolorizing textile wastewater owing to its effectiveness, affordability, operational simplicity and minimal sludge generation [6]. Numerous low-cost adsorbents, including rice husk [7], sugarcane bagasse [8], sawdust [9], coffee waste [10], zeolite [11],coconut shells [12] and fish scales [13], have shown promising results. Nonetheless, enhancing adsorption capacity through surface modification remains a key area of research.

Recently, researchers focused on incorporating nanoparticles such as TiO_2, ZnO, and Fe_3O_4 to improve surface activity and pollutant selectivity [14], [15], [16]. These nano-enhanced adsorbents benefit from high surface area, porosity, and active site availability. However, optimizing multivariable interactions such as dose, time, and agitation remains complex. To address this, statistical tools like Response Surface Methodology (RSM) offer a more efficient route to process optimization [17] . The novelty of this work lies in combining agro-waste valorization with nanotechnology to create a TiO_2-modified PKS adsorbent for Malachite Green Dye (MGD) removal. Unlike traditional adsorbents, the PKS–TiO_2 system demonstrates both sustainable material sourcing and enhanced adsorption efficiency. The integration of RSM optimization with kinetic, thermodynamic, and reusability assessments further strengthens its scientific contribution by providing a comprehensive evaluation of its performance and industrial relevance. This study aims to develop and characterize a TiO_2 nanoparticle-modified palm kernel shell (PKS)-based nano-adsorbent for the efficient removal of Malachite Green (MG) dye from textile wastewater. The work endeavors to optimize the adsorption process using Response Surface Methodology (RSM) and to evaluate the adsorbent's performance in terms of adsorption kinetics, thermodynamics, and reusability.

2. Research and Methodology

2.1 Materials

Palm kernel shells (PKS) and *Cola nitida* pods were sourced from a farm in Ede, Osun State, while wastewater was collected from a textile facility in Osogbo, Osun state, Nigeria. Analytical-grade chemicals (NaOH, KOH, HNO_3, HCl) were obtained from Sigma-Aldrich and used without further purification. Key equipment included a UV–vis spectrophotometer (Spectrum Lab 7525), FTIR spectrometer (Varian 660), muffle furnace (Carbolite ELF 11/68), and water bath shaker.

2.2 Synthesis of TiO_2 Nanoparticles

TiO_2 nanoparticles were synthesized via a green route using *Cola nitida* pod extract as a reducing agent. A mixture of 1 g pod powder and 100 mL distilled water was heated at 60 °C for 1 hour, centrifuged, and filtered. The extract (10 mL) was added to 80 mL of 5 mM TiO_2 precursor under stirring. A color change from white to light brown indicated nanoparticle formation. UV–vis absorbance at 380 nm confirmed synthesis. After 24 h incubation, the nanoparticles were dried at 100 °C for 7 h. Details on the synthesis and characterization of the nanoparticles can be found in literature [18].

2.3 Preparation of Activated Carbon from PKS

The PKS were washed, oven-dried at 70 °C for 48 h, and ground to 1–2 mm particles. Chemical activation was performed by soaking 30 g of PKS in 100 mL of 0.5 M NaOH for 12 h. The mixture was decanted, oven-dried, and carbonized at 550 °C for 2 h in a muffle furnace. The resultant material was washed to neutral pH and dried at 120 °C for 4 h [19]. 1 g/L stock solution of malachite green dye (MGD) was prepared and serially diluted to 100-500 mg/L concentrations. Absorbance was measured at 620 nm using a UV–vis spectrophotometer, and a calibration curve was generated [22].

2.4 Impregnation of PKSAC with TiO_2-NPs

To prepare the nanocomposite (PKSAC-TiO_2-NPs), 5 g of activated carbon was stirred with 100 mL TiO_2 nanoparticle solution for 12 h. The slurry was dried at 110 °C. The dried sample was then weighed, and the percentage yield of the produced PKSAC-TiO_2-NPs was evaluated using Equation 1.

$$\text{Percentage yield } (\%) = \frac{\text{final mass (g)}}{\text{inital mass (g)}} \times 100 \quad (1)$$

2.5 Product characterization

Standard ASTM procedures were used to evaluate moisture, ash, volatile matter, and fixed carbon contents. Bulk density was measured using a 10 mL graduated cylinder. Fixed carbon was calculated by subtracting moisture, ash, and volatile content from 100%. Fourier Transform Infrared Spectroscopy (FTIR) was used to determine the functional group on the adsorbent [20].

2.6 Batch Adsorption and Model Evaluation

Batch experiments were designed using the Box-Behnken model (Design Expert v13). Parameters varied were dosage (0.5-2.5 g), time (30-150 min), agitation (100-300 rpm), and temperature (30-60 °C) [9]. After treatment, the efficiency of MG dye removal was calculated using Equation 2, Where C_o and C_e are the initial and equilibrium concentrations (mg/L), respectively. Root Mean Square Error (RMSE) was used to evaluate model fit. A low RMSE value indicates good consistency between measured values and those predicted by the model, while a high RMSE signifies a significant deviation. RMSE was evaluated using Equation 3. Where $q_{e,exp}$ and $q_{e,calc.}$ Re-experimental and predicted adsorption capacities, and n is the number of data points.

$$\text{Removal efficiency } (\%\ \text{R}) = \frac{(C_o - C_e)}{C_o} \times 100 \quad (2)$$

$$\text{RMSE} = \frac{1}{n-2}\sqrt{\sum_{i=1}^{n}\left(q_{e,exp} - q_{e,calc}\right)^2} \quad (3)$$

2.7 Regeneration and Reusability

Regeneration was assessed using distilled water, 0.1 M HNO_3, and 0.1 M NaOH as desorbing agents. After each adsorption cycle under optimal conditions, the spent adsorbent was rinsed, dried at 80 °C, and reused for five cycles. Desorption efficiency was calculated to assess performance retention using Equation 4.

$$\text{Desorption } (\%) = \frac{\text{amount of MG dye desorbed}}{\text{amount of MG dye adsorbed}} \times 100 \quad (4)$$

3. Results and Discussion

3.1 Physicochemical Properties of PKSAC-TiO2-NPs

The proximate analysis (Table 1) shows a marked increase in fixed carbon content from 24.3% to 69.5% after activation, carbonization and TiO_2 nanoparticle loading. This indicates effective activation. Moisture and volatile matter decreased, while ash content increased due to modification with nanoparticles. A rise in bulk density (0.8165 to 0.8631 g/cm^3) suggests better adsorption packing [24], [25], [26].

Table 1. Physicochemical properties of produced PKSAC-TiO_2-NPs

Proximate analysis	Raw PKS	PKSAC-TiO_2-NPs
Moisture content (%)	7.80	4.90
Ash content (%)	3.6	7.6
Volatile content (%)	64.30	18.00
Fixed carbon (%)	24.30	69.50
Bulk density (g/cm3)	0.8165	0.8631
Yield (%)	-	73.5

3.2 Fourier Transform Infrared Spectroscopy Analysis

Fourier-transform infrared analysis of the PKSAC-TiO_2-NPs was conducted using a Shimadzu FTIR-8400S spectrophotometer across 500-4000 cm^{-1}. FTIR spectra (Figure 1) displayed peaks for key functional groups. O–H stretching appeared around 3200-3500 cm^{-1}, and C=O stretching was noted at 1697 cm^{-1}. Post-adsorption shifts, including a move from 1404 to 1427 cm^{1} for O-H bending, indicated interaction between MG dye and surface site [7], [13].

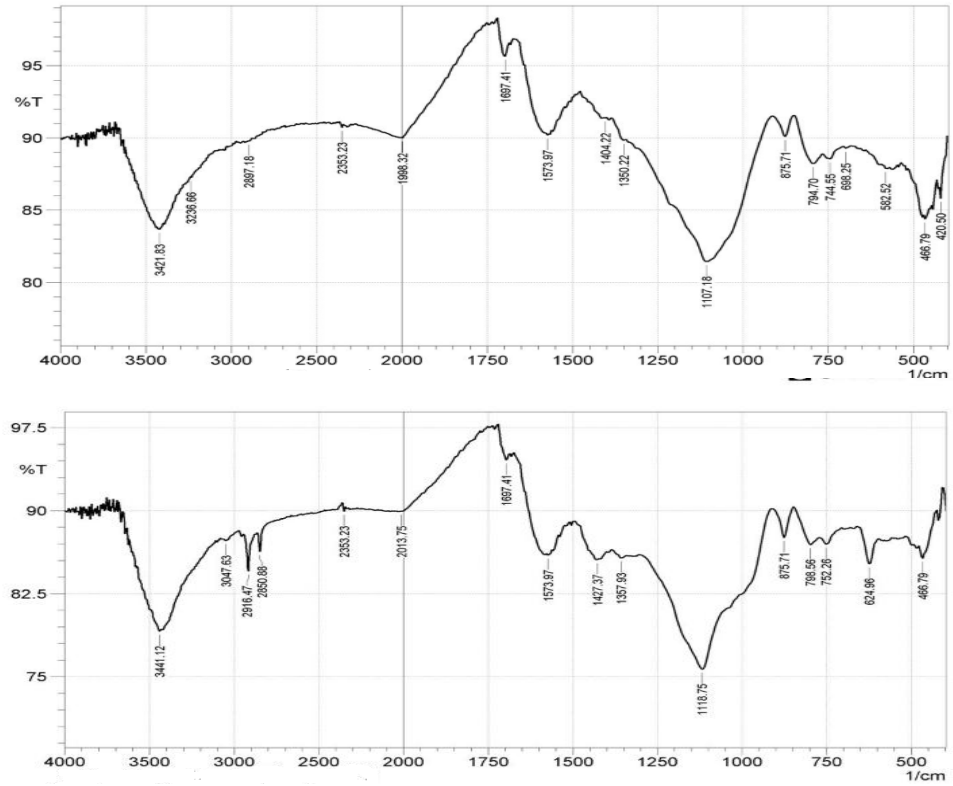

Figure 1. FTIR spectra of PKSAC-TiO_2-NPs (a) before (b) after adsorption

3.3 Calibration Curve

MGD solutions with concentrations from 100 to 500 mg/L were prepared, and their absorbance values were measured using a UV-Visible spectrophotometer. MG dye concentrations (100–500 mg/L) yielded a strong linear relationship with absorbance (R^2 = 0.9939), confirming the spectrophotometric method's accuracy (Figure 2).

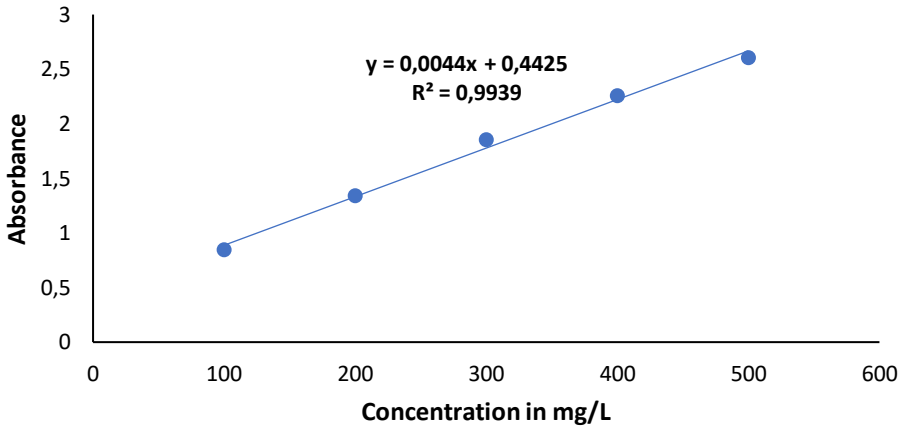

Figure 2. Calibration curve

3.4 Batch Adsorption Experiments

Across 29 experimental runs, removal efficiency varied from 51.7% to 93.26% (Table 2). The relationship between process variables and % R fit the quadratic model best, as illustrated in Equation 10. The statistical evaluation indicated that the terms A, B, C, D, AB, BD, CD, B^2, C^2, and D^2 had a significant influence on the response while BC was insignificant for MG dye removal (Table 3). The model demonstrated strong reliability, evidenced indicated by the high coefficient of determination (R^2 = 0.997). Maximum efficiency occurred at 2.5 g dosage, 150 min, and 45 °C. ANOVA confirmed dosage, time, and temperature as significant factors ($p < 0.05$), while agitation had a minor negative influence.

Table 2. Removal efficiency of MG Dye using PKSAC-TiO_2-NPs

Run	Adsorbent dosage (g)	Contact time (min)	Agitation rate (rpm)	Temperature (°C)	Removal efficiency (%)
1	1.5	30	100	45	64.04
2	0.5	30	200	45	57.52
3	1.5	30	200	60	65.5
4	0.5	90	200	60	61.2
5	1.5	90	100	30	68.6
6	1.5	150	100	45	80.7
7	0.5	150	200	45	63.17
8	2.5	90	100	45	89.7
9	1.5	90	200	45	71.3
10	0.5	90	300	45	58
11	1.5	30	300	45	66.3
12	1.5	90	200	45	71.6
13	1.5	90	200	45	71.4
14	1.5	150	200	30	74.7
15	1.5	30	200	30	61.3
16	2.5	90	300	45	90.6
17	0.5	90	200	30	51.7
18	1.5	90	200	45	71.5
19	1.5	150	300	45	81.8
20	1.5	90	300	60	78
21	1.5	150	200	60	82.8
22	2.5	90	200	60	92.3
23	2.5	30	200	45	83.18

24	2.5	90	200	30	86.36
25	0.5	90	100	45	55.61
26	1.5	90	100	60	73.4
27	1.5	90	300	30	73.52
28	2.5	150	200	45	93.26
29	1.5	90	200	45	71.42

$$\% R = +21.12 + 21.5868 * \text{Adsorbent dosge} + 0.2066 * \text{contact time} - 0.0396 * \text{Agitation rate} + 0.1661 * \text{Temperature} - 0.0489 * \text{Adsorbent dosage} * \text{contact time} - 0.000048 * \text{contact time} * \text{agitation rate} + 0.00082 * \text{contacttime} * \text{temperature} - 0.000975 * \text{Agitationrate} * \text{Temperature}$$

Table 3. Analysis of Variance (ANOVA) for removal of MG dye using PKSAC-TiO_2-NPs

Source	Sum of Squares	df	Mean Square	F-value	p-value
Model	2905.68	11	264.15	3576.72	< 0.0001
Adsorbent dosage (A)	1937.59	1	1937.59	26235.54	< 0.0001
Contact time (B)	371.3	1	371.3	5027.54	< 0.0001
Agitation rate (C)	6.56	1	6.56	88.76	< 0.0001
Temperature (D)	48.76	1	48.76	660.22	< 0.0001
AB	12.85	1	12.85	173.96	< 0.0001
BC	0.3364	1	0.3364	4.55	0.0586
BD	1.24	1	1.24	16.85	0.0021
CD	3.28	1	3.28	44.43	< 0.0001
B^2	1.21	1	1.21	16.43	0.0023
C^2	19.72	1	19.72	267.06	< 0.0001
D^2	0.6263	1	0.6263	8.48	0.0155
Residual	0.7385	10	0.0739		
Lack of Fit	0.6278	6	0.1046	3.78	0.1094
Pure Error	0.1107	4	0.0277		
Cor Total	2906.42	21			

*Values of "Prob > F" less than 0.0500 indicate model terms are significant.

3.5 Interactive Effects of Parameters

Response surface plots (Figure 3a) demonstrate that increasing both the adsorbent dosage and contact time positively influenced malachite green (MG) dye removal. As shown in Figure 3b, prolonged contact time and moderate agitation rates further enhanced removal efficiency. However, excessively high agitation appeared to reduce performance slightly, likely due to desorption effects. Figure 3c highlights that elevated temperatures, when combined with longer contact durations, also promoted better dye removal. Figure 3d illustrates the interaction between agitation rate and temperature, indicating that while both parameters are influential, very high agitation may cause a marginal decrease in efficiency. This decline could be attributed to the re-release of adsorbed dye molecules or reduced interaction time between the dye and the adsorbent. Although increased agitation improves dye transport, excessive turbulence may disrupt effective adsorption on the adsorbent surface.

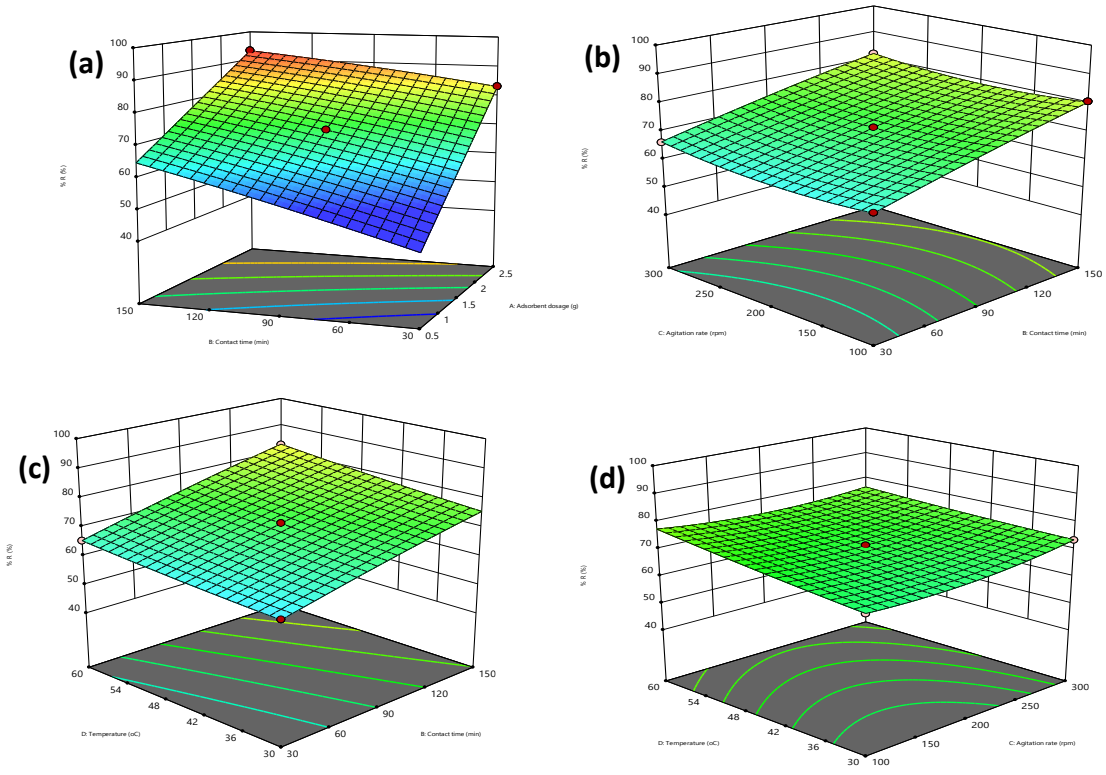

Figure 3. 3D response surface plots on effect of (a) adsorbent dosage and contact time (b) contact time and agitation rate (c) contact time and temperature (d) agitation rate and temperature on dye removal

3.6 Process Optimization

Numerical optimization was carried out to determine the optimum adsorbent dosage, contact time, agitation rate and temperature to achieve maximum dye removal using PKSAC-TiO_2-NPs. The optimized conditions were: 2.28 g dosage, 142 min time, 279 rpm, and 58°C. Predicted (93.8%) and experimental (92.6%) removal rates showed close agreement, with only 1.38% error. Comparable, RSM-based studies in the last decade report similar or higher peak removals under different matrices and designs: MgO-impregnated clays and nano-bentonite optimized via RSM achieved 92 to 94.5% with robust multi-cycle reuse, confirming that nano-enhancement and statistical tuning reliably elevate performance [28]. Likewise, Box–Behnken optimization on *Rumex abyssinicus* activated carbon reached up to 99.9% removal while validating PSO kinetics and favorable thermodynamics, reinforcing the consistency between optimized operating windows and mechanism assignments across systems [29].Recent DOE/RSM work on almond-shell carbon waste also demonstrates that structured optimization efficiently navigates multi-factor spaces to identify high-removal regimes for MG, aligning with the approach and outcome reported [30].

3.7 Model Validation

To confirm the accuracy of the optimization model, validation was conducted by comparing the predicted MG dye removal efficiency with the experimentally obtained value. The results showed a small error margin of 1.38%, as presented in Table 4. The closeness between predicted and experimental values confirms the reliability and robustness of the developed model for accurately predicting MG dye removal efficiency under the optimized conditions.

Table 4. Model validation of malachite dye green removal using PKSAC-TiO_2-NPs

Adsorbent dosage (g)	Contact time (min)	Agitation rate (rpm)	Temperature (℃)	Removal Efficiency of dye (%)		Error (%)
				Predicted	Experimental	
2.28	142	279	58	93.80	92.60	1.38

3.8 Regeneration and Reusability Study of spent PKSAC-TiO_2-NPs

The regeneration performance of PKSAC–TiO_2–NPs was evaluated using distilled water, 0.1 M HNO_3, and 0.1 M NaOH as desorbing agents across five adsorption–desorption cycles (Table 5). Among the solvents, NaOH showed the highest regeneration efficiency, with only a slight decrease from 94.6% to 92.3% after five cycles. Distilled water and HNO_3 also enabled recovery of adsorption capacity, albeit with slightly lower retention. The minor decline in performance was attributed to pore blockage and gradual surface degradation of active sites during repeated use. These outcomes are consistent with observations in the literature: tea stalk powder maintained >95% efficiency after six NaOH regenerations, reflecting excellent retention [31]; alkaline regenerants, especially NaOH, are noted for preserving active sites better than acids [32]; and a TiO_2/biochar composite sustained its removal performance over five cycles with no observable loss [33]. Altogether, these comparisons confirm that PKSAC–TiO_2–NPs performs within the upper range of low-cost adsorbents for repeated dye removal.

Conclusively, the combination of strong regeneration ability and the sustainable origin of palm kernel shell makes PKSAC–TiO_2–NPs highly suitable for scalable industrial dye remediation applications

Table 5. Regeneration and Reusability Results for PKSAC-TiO_2-NPs

Regeneration cycle	Removal efficiency (%)	Distilled water	
		HNO_3	NaOH
1st cycle	92.50	91.80	94.60
5th cycle	91.80	89.63	92.30

3.9 Evaluation of Kinetic Parameters for MG Removal using PKSAC-TiO_2- Nanocomposite

Figure 4 illustrates the kinetic plots based on the application of Pseudo-first-order (PFO) and Pseudo-second-order (PSO) models to describe MG dye adsorption onto PKSAC-TiO_2-NPs. The pseudo-second-order kinetic model provided the best fit (R^2 = 0.989; RMSE = 0.0005), indicating chemisorption. In contrast, the pseudo-first-order model had lower correlation (R^2 = 0.80). Furthermore, the experimental q_e ($q_{e,exp}$) presented in Table 6 is closer to the calculated q_e ($q_{e,cal}$) for the PSO model. Therefore, the PSO kinetic model with the highest R^2 value and the lowest RMSE best describe the adsorption process.

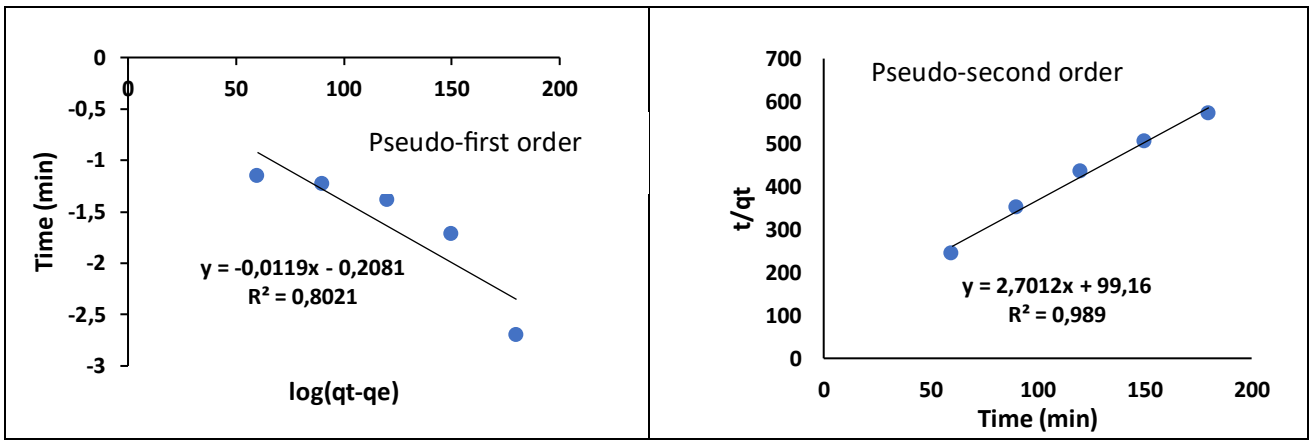

Figure 4. Kinetic plot of malachite dye green removal using PKSAC-TiO_2-NPs

Table 6. Kinetics parameters of adsorption of malachite dye using PKSAC-TIO_2-NPs

Kinetic model	Unit	Value
Pseudo-first order		
K_1	h^{-1}	0.027
$q_{e,exp}$	mg/g	0.33
$q_{e,cal}$	mg/g	0.62
R^2	----	0.8021
RMSE	----	0.0970
Pseudo-second order		
K_2	g/(mgmin)	0.074
$q_{e,exp}$	mg/g	0.33
$q_{e,cal}$	mg/g	0.37
R^2	----	0.9890
RMSE	----	0.0005

3.10 Thermodynamic study of Malachite Green Dye Removal using PKSAC-TiO_2-NPs

Figure 5 presents the thermodynamic plot for Malachite Green (MG) dye adsorption onto PKSAC-$Ti0_2$-NPs. Negative ΔG^0 values confirmed spontaneous adsorption. A positive ΔH^0 (18.61 kJ/mol) suggested endothermic nature, while positive ΔS^0 indicated increased molecular randomness at the solid–liquid interface (Table7). According to adsorption energy classifications, energies in the range of 4-10 kJ/mol are indicative of van der Waals interactions, while values around 5 kJ/mol suggest hydrophobic interactions. Hydrogen bonding is typically associated with energies between 2-40 kJ/mol, and dipole-dipole interactions generally occur within the 2.29 kJ/mol range. The adsorption enthalpy (ΔH°) value of 18.61 kJ/mol obtained revealed that the process is likely governed by physical adsorption mechanisms, including hydrogen bonding and dipole interactions [34]. Moreover, the decline in ΔG° values with rising temperature suggests that the adsorption process becomes increasingly favorable, reinforcing its endothermic character.

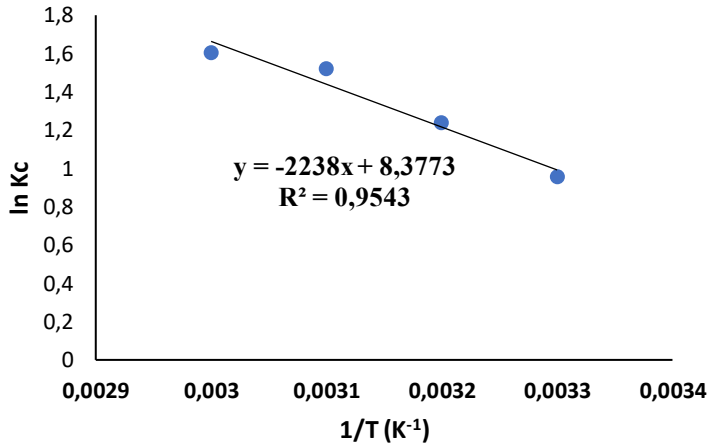

Figure 5. Thermodynamic study of malachite dye green removal using PKSAC-TiO_2-NPs

Table 7. Thermodynamic parameters of adsorption of malachite dye using PKSAC-TiO_2-NPs

Temp. (K)	ΔH^0 $(\frac{KJ}{mol})$	ΔS^0 $(KJK^{-1}mol^{-1}$	ΔG^0 $(\frac{KJ}{mol})$
303	18.61	0.6965	-2.497
313			-3.193
323			-3.890
333			-4.586

3.11 Comparative Analysis of Malachite Green Dye Removal Using Various Adsorbents

Compared to other adsorbents as presented in Table 8, PKSAC-TiO_2-NPs offered competitive efficiency, strong reusability, and economic feasibility. While certain materials reached >99% removal, this nanocomposite balances cost-effectiveness with high removal capacity, making it viable for real-world wastewater treatment.

Table 8. Comparison of results with literature

Adsorbent	Removal efficiency (%R)	Kinetic model	Thermodynamic model	References
Wood apple	98.87	Pseudo-second order	Endothermic, spontaneous	[35]
Rice husks	95.70	Pseudo-second order	Exothermic, spontaneous	[36]
Zinc tungsten	75.00	Pseudo-second order	Endothermic, spontaneous	[37]
Rumex abyssinicus	99.90	Pseudo-second order	Endothermic, spontaneous	[29]
Nano- bentonite	98.00	Pseudo-first order	Exothermic, non-spontaneous	[28]
MgO-impregnated clay	90.00	Pseudo-first order	Exothermic, spontaneous	[28]
Porous organic polymer	99.60	Elovich model	Endothermic, spontaneous	[38]
PKSAC-TiO_2-NPs	92.60	Pseudo-second order	Endothermic, spontaneous	This study

4. Conclusion

This study demonstrates that palm kernel shell-derived activated carbon modified with TiO_2 nanoparticles (PKSAC–TiO_2-NPs) is an effective and sustainable adsorbent for malachite green dye (MGD) removal. Characterization confirmed its favorable surface properties, while RSM optimization achieved a maximum removal efficiency of 92.6%**.** The adsorption process followed pseudo-second-order kinetics and was spontaneous and endothermic, with reusability tests showing stable performance over several cycles. Compared with other agro-waste and nano-enhanced adsorbents, PKSAC–TiO_2-NPs balanced low cost with improved functionality. Overall, this work contributes a practical and scalable solution for textile wastewater treatment. Its novelty lies in valorizing palm kernel shell into a TiO_2-modified nano-adsorbent that integrates sustainable resource use with enhanced adsorption performance. Future studies should explore pilot-scale application, regeneration economics, and multi-contaminant removal to advance industrial deployment.

Author contributions: Olowonyo Idayat A.: curated data, carried out the experiment, acquired funding, and contributed to writing and editing. **Sole-Adeoye Opeoluwa D.**: methodology, validated results, and assisted in manuscript review. **Salam Kazeem K.:** designed the methodology, validated results, and assisted in manuscript review. **Aremu Mujidat O.**: curated and analyzed the data. **Akinwumi Odunayo D.**: curated and analyzed the data. **Oreofe Toyin A.**: original draft preparation. **Owolabi Stephen O.**: original draft preparation.

Acknowledgement: Acknowledgments may be directed to individuals or institutions that have contributed to the research or a government agency, or This research received no specific grant from any funding agency in the public, commercial, or not-for-profit sectors.

Conflict of Interest: The authors declare that there are no conflicts of interest.

5. References

[1] O. A. A. Eletta *et al.*, “Valorisation of Cocoa (Theobroma cacao) pod husk as precursors for the production of adsorbents for water treatment,” vol. 2515, 2020, doi: 10.1080/21622515.2020.1730983.

[2] M. A. D. Flores *et al.*, “Efficient Dye Removal from Real Textile Wastewater Using Orange Seed Powder as Suitable Bio-Adsorbent and Membrane Technology,” *Water*, vol. 14, 2022.

[3] P. V. Gayathri, S. Yesodharan, and E. P. Yesodharan, “Microwave/Persulphate assisted ZnO mediated photocatalysis (MW/PS/UV/ZnO) as an efficient advanced oxidation process for the removal of RhB dye pollutant from water,” *J. Environ. Chem. Eng.*, vol. 7, no. 4, p. 103122, 2019, doi: 10.1016/j.jece.2019.103122.

[4] R. Javeed Ganaie, S. Rafiq, and A. Sharma, “Recent Advances in Physico-chemical Methods for Removal of Dye from Wastewater,” *IOP Conf. Ser. Earth Environ. Sci.*, vol. 1110, no. 1, 2023, doi: 10.1088/1755-1315/1110/1/012040.

[5] A. M. S. Solano, C. A. Martínez-Huitle, S. Garcia-Segura, A. El-Ghenymy, and E. Brillas, “Application of electrochemical advanced oxidation processes with a boron-doped diamond anode to degrade acidic solutions of Reactive Blue 15 (Turqueoise Blue) dye,” *Electrochim. Acta*, vol. 197, pp. 210–220, 2016, doi: 10.1016/j.electacta.2015.08.052.

[6] V. Mei and R. Mohd, “Adsorption of methylene blue from aqueous solution using palm kernel shell activated carbon Adsorption of Methylene Blue from Aqueous Solution using Palm Kernel Shell Activated Carbon,” *AIP Conf. Proc.*, vol. 020038, p. 2068, 2019, doi: 10.1063/1.5089337.

[7] M. L. Firdaus, N. Krisnanto, W. Alwi, R. Muhammad, and M. A. Serunting, “Adsorption of Textile Dye by Activated Carbon Made from Rice Straw and Oil Palm Midrib,” *Aceh Int. J. Sci. Technol.*, vol. 6, no. 1, pp. 1–7, 2017, doi: 10.13170/aijst.6.1.5502.

[8] K. Sharma, T. K. Shinha, N. Katare, and N. Bansod, “Removal of Dyes from Textile Industrial Wastewater using Sugarcane Bagasse,” *Int. J. Text. Eng. Process.*, vol. 4, no. 3, pp. 2–6, 2018.

[9] O. Eletta, S. I. Mustapha, O. Ajayi, and A. T. Ahmed, “Optimization of Dye Removal from Textile Wastewater using Activated Carbon from Sawdust,” *Niger. J. Technol. Dev. ·*, no. March, 2018, doi: 10.4314/njtd.v15i1.5.

[10] S. Wong, Y. Lim, N. Ngadi, and R. Mat, “Removal of acetaminophen by activated carbon synthesized from spent tea leaves: equilibrium, kinetics and thermodynamics studies,” *Powder Technol.*, p. #pagerange#, 2018, doi: 10.1016/j.powtec.2018.07.075.

[11] S. M. Turp, G. A. Turp, N. Ekinci, and S. Özdemir, “Enhanced adsorption of methylene blue from textile wastewater by using natural and artificial zeolite,” *Water Sci. Technol.*, vol. 82, no. 3, pp. 513–523, 2020, doi: 10.2166/wst.2020.358.

[12] V. B. Mane, S. Benkar, S. Bhavsar, and A. Bandhankar, “Removal of Dye From Wastewater Using Agricultural Waste As Low,” *J. Emerg. Technol. Innov. Res.*, vol. 7, no. 9, pp. 404–414, 2020.

[13] R. A. Jahan, M. M. Hassan, A. A. Rana, and M. M. Karim, “Adsorption of Anionic and Cationic Dyes from Textile Effluents by Activated Carbon Prepared from Sawdust and Fish Scale,” *Adv. Chem. Eng. Sci.*, vol. 13, no. 03, pp. 189–202, 2023, doi: 10.4236/aces.2023.133014.

[14] S. Enahoro, A. Kazeem, K. Salam, A. Olanrewaju, A. Micheal, and A. Oyelakin, “Adsorptive desulfurization of diesel with modified pig dung : experimental design with optimization , kinetics , isotherms and thermodynamics studies,” *Discov. Appl. Sci.*, 2024, doi: 10.1007/s42452-024-05859-5.

[15] T. Assefa and F. Mazengiaw, “Iron-based nanoparticles in wastewater treatment : A review on synthesis methods , applications , and removal mechanisms,” *J. Saudi Chem. Soc.*, vol. 25, no. 8, p. 101280, 2021, doi: 10.1016/j.jscs.2021.101280.

[16] M.O. Aremu , Salam K.K , Olowonyo, I.A., Lateef, A., “Applications of Nanoadsorbent Technology in Treatment of Industrial Wastewater: A mini Review,” *Nanoplus Sci. Technol. Nanomater.*, vol. 4, pp. 16–26, 2022.

[17] T. Jamil *et al.*, “Bentonite-Clay/CNT-Based Nano Adsorbent for Textile Wastewater Treatment: Optimization of Process Parameters,” *Water (Switzerland)*, vol. 15, no. 18, 2023, doi: 10.3390/w15183197.

[18] I. A. Olowonyo, K. kolapo Salam, M. O. Aremu, and A. Lateef, “Synthesis , characterization , and adsorptive performance of titanium dioxide nanoparticles modified groundnut shell activated carbon on ibuprofen removal from pharmaceutical wastewater,” *Waste Manag. Bull.*, 2023, doi: 10.1016/j.wmb.2023.11.003.

[19] M. Adib, M. Razi, A. Al-gheethi, and M. Al-qaini, “Efficiency of activated carbon from palm kernel shell for treatment of greywater,” *Arab J. Basic Appl. Sci.*, vol. 0, no. 0, pp. 1–8, 2018, doi: 10.1080/25765299.2018.1514142.

[20] V. . Onwukeme and C. . Egemba, “REMOVAL OF SILVER AND CADMIUM FROM INDUSTRIAL WASTE WATER USING CHEMICALLY MODIFIED PALM KERNEL SHELLS,” *J. Chem. Socety*, vol. 47, no. 6, pp. 1335–1347, 2022.

[21] O. A. Ekpete, A. C. Marcus, and V. Osi, “Preparation and Characterization of Activated Carbon Obtained from Plantain (Musa paradisiaca) Fruit Stem,” *J. Chem.*, vol. 2017, p. Hindawi Journal of Chemistry, 2017.

[22] B. Mughal, S. Zohaib, J. Zaidi, and X. Zhang, “applied sciences Biogenic Nanoparticles : Synthesis , Characterisation and Applications,” 2021.

[23] O. A. A. Eletta, S. I. Mustapha, O. A. Ajayi, and A. T. Ahmed, “Optimization of Dye Removal from Textile Wastewater using Activated Carbon from Sawdust,” *Niger. J. Technol. Dev.*, vol. 15, no. 1, pp. 26–32, 2018.

[24] O. O. E. Onawumi, A. A. Sangoremi, and O. S. Bello, “Preparation and characterization of activated carbon from groundnut and egg shells as viable precursors for adsorption,” *J. Appl. Sci. Environ. Manag.*, vol. 25, no. 9, pp. 1707–1713, 2021, doi: 10.4314/jasem.v25i9.24.

[25] S. M. Anisuzzaman, N. Sinring, and R. Fran Mansa, “Properties Tuning of Palm Kernel Shell Biochar Granular Activated Carbon Using Response Surface Methodology for Removal of Methylene Blue,” *J. Appl. Sci. Process Eng.*, vol. 8, no. 2, pp. 1002–1019, 2021, doi: 10.33736/jaspe.3961.2021.

[26] M. O. Aremu, A. O. Arinkoola, I. A. Olowonyo, and K. K. Salam, “Improved phenol sequestration from aqueous solution using silver nanoparticle modi fi ed Palm Kernel Shell Activated Carbon,” *Heliyon*, vol. 6, no. May, p. e04492, 2020, doi: 10.1016/j.heliyon.2020.e04492.

[27] A. A. Pam, A. H. Abdullah, Y. P. Tan, and Z. Zainal, “Physicochemical properties of porous activated carbon prepared from palm kernel shell through a low-cost activation protocol,” *S. Afr. J. Sci.*, vol. 118, no. 9–10, pp. 1–7, 2022, doi: 10.17159/sajs.2022/13497.

[28] M. Taha and M. Hussien, “Optimization study of the adsorption of malachite green removal by MgO nano - composite , nano - bentonite and fungal immobilization on active carbon using response surface methodology and kinetic study,” *Environ. Sci. Eur.*, pp. 1–37, 2023, doi: 10.1186/s12302-023-00728-1.

[29] M. Abewaa, A. Mengistu, T. Takele, J. Fito, and T. Nkambule, “Adsorptive removal of malachite green dye from aqueous solution using Rumex abyssinicus derived activated carbon,” *Sci. Rep.*, pp. 1–16, 2023, doi: 10.1038/s41598-023-41957-x.

[30] F. Chouli, A. O. Ezzat, L. Sabantina, A. Benyoucef, and A. Zehhaf, “Optimization Conditions of Malachite Green Adsorption onto Almond Shell Carbon Waste Using Process Design,” *Molecules*, vol. 29, no. 1, pp. 1–16, 2024, doi: 10.3390/molecules29010054.

[31] X. Liu *et al.*, “Adsorption of Malachite Green from Aqueous Phase by Tea Stalk Powder: Parameters, Kinetic, Isothermal, and Thermodynamic Studies,” 2023, *BioResources 18(3),*.

[32] T. Alsawy, E. Rashad, M. El-Qelish, and R. H. Mohammed, “A comprehensive review on the chemical regeneration of biochar adsorbent for sustainable wastewater treatment,” *npj Clean Water*, vol. 5, no. 1, 2022, doi: 10.1038/s41545-022-00172-3.

[33] A. Mancuso *et al.*, “Ball–milled TiO2/biochar hybrid system as a heterogeneous photocatalyst for tannery dyes removal in aqueous solution,” *J. Mol. Liq.*, vol. 399, no. March, p. 124357, 2024, doi: 10.1016/j.molliq.2024.124357.

[34] M. Sajid *et al.*, “Adsorption characteristics of paracetamol removal onto activated carbon prepared from Cannabis sativum Hemp,” *Alexandria Eng. J.*, vol. 61, no. 9, pp. 7203–7212, 2022, doi: 10.1016/j.aej.2021.12.060.

[35] A. S. Sartape, A. M. Mandhare, V. V. Jadhav, P. D. Raut, M. A. Anuse, and S. S. Kolekar, “Removal of malachite green dye from aqueous solution with adsorption technique using Limonia acidissima (wood apple) shell as low cost adsorbent,” *Arab. J. Chem.*, vol. 10, no. April 2015, pp. S3229–S3238, 2017, doi: 10.1016/j.arabjc.2013.12.019.

[36] V. M. Muinde, J. M. Onyari, B. Wamalwa, J. Wabomba, and R. M. Nthumbi, “Adsorption of Malachite Green from Aqueous Solutions onto Rice Husks: Kinetic and Equilibrium Studies,” *J. Environ. Prot. (Irvine,. Calif).*, vol. 08, no. 03, pp. 215–230, 2017, doi: 10.4236/jep.2017.83017.

[37] H. Ladio, J. Oladejo, A. Saka, T. Chinedu, M. Abdullahi, and S. Mustapha, “Heliyon Effective removal of malachite green from local dyeing wastewater using zinc-tungstate based materials,” *Heliyon*, vol. 9, no. 9, p. e19167, 2023, doi: 10.1016/j.heliyon.2023.e19167.

[38] S. Melhi *et al.*, “Effective Removal of Malachite Green Dye from Water Using Low-Cost Porous Organic Polymers: Adsorption Kinetics, Isotherms, and Reusability Studies,” *Water (Switzerland)*, vol. 16, no. 13, 2024, doi: 10.3390/w16131869.